

Application of 2D resistivity profiling for mapping and interpretation of geology in a till aquitard near Luck Lake, Southern Saskatchewan, Canada

Khaled S. Gemail

Received: 3 April 2013 / Accepted: 13 June 2014 / Published online: 6 July 2014
© Springer-Verlag Berlin Heidelberg 2014

Abstract In Southern Saskatchewan, Canada, the clay-rich till deposits are important as sites for waste disposal and as protective covers on regional aquifers due to their low hydraulic conductivity and great thickness. In such case, it is very important to fully understand the detailed distribution and the variation of the gravel areas in the glacial cap to study the infiltration speed in the subsoil. Resistivity measurements in the form of 1D Schlumberger sounding and 2D Wenner resistivity profiling were carried out in the area north of Luck Lake, Southern Saskatchewan, to map the extent of gravel substratums in the till cap and to investigate the impact of a known fault on the gravel and till in the area. These measurements were controlled with depth and single point resistivity information from two boreholes drilled previously. The analysis of the 2D inverted sections shows the importance of electrical resistivity techniques for mapping the lateral and vertical heterogeneities in the till deposits, which are related to the hydraulic processes controlling groundwater recharge. The 2D resistivity imaging sections show the major till units on both sides of the east–west fault system. The strong resistivity contrast between the upper part of the till (10–23 Ωm) and the basal part ($>150 \Omega\text{m}$) allows the mapping of a gravel layer in the lower parts. This gravel substratum is better defined and more significant towards the ridge in the northern area due to its greater thickness and higher resistivity. The lowland area is characterized by clay-rich of glaciolacustrine deposits identified in a borehole and by low resistivities ($<20 \Omega\text{m}$). The resistivity of the Cretaceous mudstone bedrock is low, typically $<10 \Omega\text{m}$. No gravel deposits are interpreted to the downside of the fault.

Keywords Luck Lake · Saskatchewan · 2D Resistivity imaging · Quaternary · Intertill gravel · Glaciolacustrine

Introduction

The occurrence and movement of the groundwater and surface pollutants in glacial deposits are influenced by different factors, such as surface topography, clay content, fracture system, faults and nature of weathering. Canadian Prairie tills tend to be distinguished and mapped using a combination of geophysical well-log signature, clay contents, presence of intervening of weathering profiles, and presence of sand and gravel layers or boulders pavements (Christiansen 1986; Cummings et al. 2012). Correlation of lithology and fractures sets between core holes or wells is difficult in till because of heterogeneous characteristics inherent in most glacial sediments (Haefner 2000).

The glacial deposits in Southern Saskatchewan act as protective zone for waste disposal on regional aquifers. In addition, clay-rich deposits are being considered as possible hosts for disposal of high-level radioactive waste (McCombie 1997). Quantifying groundwater flow through these aquitards has implications for solute transport in aquitards and protection of underlying aquifers (Shaw and Hendry 1998). Because of the extremely long time scales for groundwater flow and contaminant transport in till aquitards (over thousands of years or even longer), these formations can function as protective barriers against contaminant transport to more potable groundwater resources and allow them to be considered as historical hydrogeologic archives of ancient climates, geologic processes, and chemistry (Remenda 1993, Hendry 1988; Hendry et al. 2003, 2005). Hendry et al. (2011) studied the vertical controls on solute transport in glacial till aquitard

K. S. Gemail (✉)
Department of Geology, Faculty of Science, Zagazig University,
Zagazig 44519, Egypt
e-mail: khaledgemail@zu.edu.eg

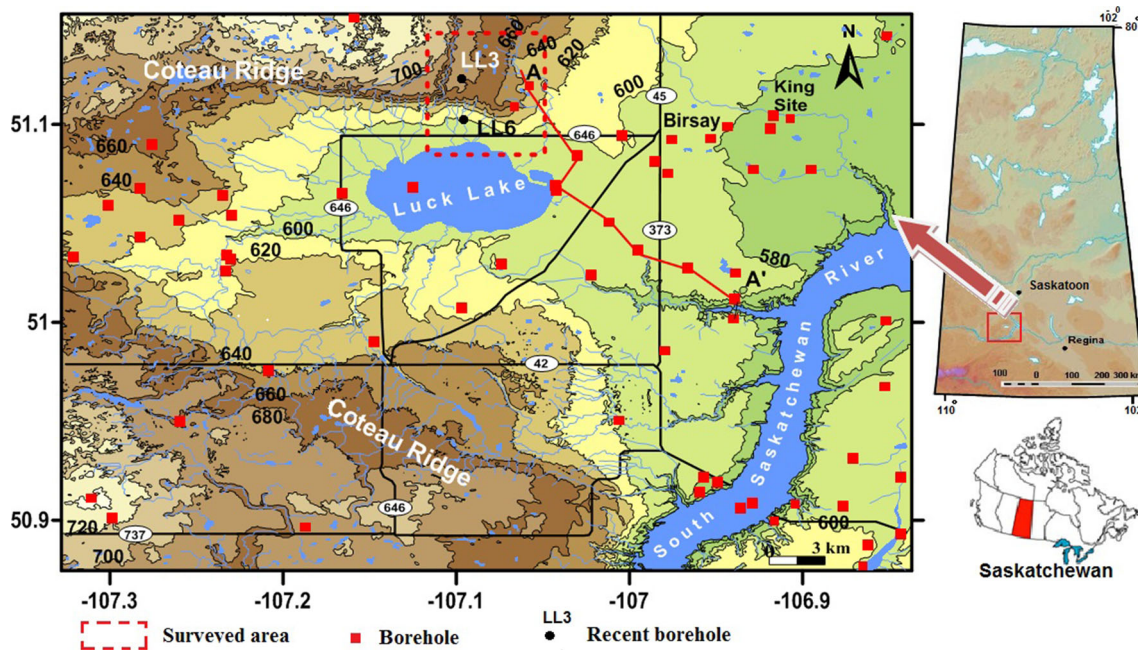


Fig. 1 Location map of the Luck Lake area shows the elevation and historic borehole distributions (Christiansen 1986); contour interval is 20 m. The red line represents the location of geologic cross section (Fig. 5). LL3 and LL6 are recent boreholes (Hendry et al. 2011)

(>120 m thick) through seven boreholes in the area around Luck Lake using a high-resolution 1D stable isotope profiles. In this case, the fracture system as well as gravel deposits in the aquitard allow fluid percolation even when the matrix itself is relatively impermeable (Phillips 2009). Geophysical surveys can apply for mapping the structural disturbances, such as fault system and layer boundaries and study its impact on solute transport in aquitard systems.

The determination of the spread of groundwater contaminations is difficult because of the high cost of drilling and the rapid changes of subsurface layer distributions, which are common in the glacial deposits' investigations. Geo-electrical resistivity techniques provide the capability of mapping the lateral and vertical subsurface variations and to characterize the subsurface continuously over larger areas between boreholes (Gemail 2012). In environmental applications, resistivity surveys are capable of mapping overburden depth, stratigraphy, faults, fracture zones, rock units, and voids (Ward 1990; Aizebeokhai 2009). Electrical methods are efficient in mapping the variations in clay-rich deposits, because clay formations show low resistivities and sandy gravel formations are related to relatively high resistivities (Gemail 2012).

This mapping process is based on the electrical resistivity distributions, which are related to the fracture pattern, clay content, and subsurface hydrogeological conditions. In a resistivity survey, an electrical current is injected into the ground through a pair of current electrodes and the produced voltage difference on a second pair of electrodes is

measured and interpreted in terms of the resistivity distribution in the ground. The obtained apparent resistivity values depend on the actual resistivity distribution, as well as the electrode spacing and type of electrode array. As glacial deposits are often complex, with abrupt lateral changes over short distances, there is a need for more detailed information across an entire site (Smith and Sjogren 2006). Electrical resistivity imaging (2D) has been widely used in environmental investigations due to the need for a high-resolution approach to delineate buried structures, gravel deposits, and in areas of complex geology, structural framework and stratigraphy (Griffiths and Barker 1993). In glacial areas, the 2D electrical resistivity tomography (ERT) can be used as a rapid sand and gravel reconnaissance tool (Chambers et al. 2012). In the King Site area, northeast of Luck Lake (Fig. 1), Boris and Merriam (2002) and Boris (2005) applied the azimuthal resistivity technique to detect the electrical anisotropy which is related to fracture direction and intensity in the till aquitard of Southern Saskatchewan.

In the Luck lake area, Southern Saskatchewan (Fig. 1), DC resistivity surveys in the form of Schlumberger soundings and Wenner 2D imaging profiles were carried out along a profile running between two boreholes LL3 and LL6 and crossing the Coteau Ridge, which is a fault zone. These surveys aim to study the effectiveness of DC resistivity method for mapping the gravels and permeable deposits in the till deposits as well as the resistivity signal of the fractures and heterogeneities in the upper part of the

till aquitard. Therefore, it is very important to fully understand the detailed distribution and the variation of the permeable zones in the clay-rich cap to study the vulnerability conditions of the lower aquifers with inhomogeneous till aquitards. The aim of the 1D survey is to map the vertical lithological sequence in the area. However, it does not take into account the horizontal changes in the till deposits. To overcome this limitation, the 2D resistivity imaging was applied and integrated with prior 1D survey, where the variations of resistivity in both vertical and horizontal directions are considered and treated within short distances.

In the present work, a theoretical model is assumed based on the obtained geological and hydrogeological information from boreholes. This model was correlated with the observed resistivity profiles to draw a clear picture of the subsurface conditions and to determine the origin and extension of the gravels in the whole area.

Study area and geological setting

The Luck Lake study area is located 120 km southwest of Saskatoon, Saskatchewan, Canada (Fig. 1). The study area is bounded on the north, west and south by a hummocky ridge called the Coteau Ridge (maximum elevation of 710 m asl) and to the east by the South Saskatchewan River basin (560 m asl). Two boreholes (LL3, 353208E, 5665835N and LL6, 13 353142E, 5663394N) were drilled along a profile crossing the Coteau Ridge (Fig. 1). These two boreholes show great variation in solute transport conditions related to the nature of the till on the both sides of Coteau Ridge (Hendry et al. 2011). At LL3, a 13-m thick gravel layer was observed at 37 m depth. No gravel was observed in the downside at LL6 to a depth of 50 m.

The area around Luck Lake, Southern Saskatchewan is covered by thick (>30 m) glacial deposits, weathered to a depth of 15 m, overlying dark gray, silty marine clay of the Snakebite Member of the Cretaceous Bearpaw Formation (Van Stempvoort and van der Kamp 2003). The basal part of the till is gray and unoxidized and overlain by a hard, jointed and stained oxidized till.

The till deposits in the Luck Lake area have been described by Christiansen (1986); Remenda (1993); Shaw and Hendry (1998); Van Stempvoort and Van der Kamp (2003) and Christiansen and Schmid (2005). The geological processes of Southern Saskatchewan glacial deposits include: (1) outwash of stratified sediments derived from melting glaciers, (2) inwash of deltaic stratified sediments deposited from extra-glacial streams, and (3) salt collapse structures which occurred during the glaciation time 20,000 years ago (Christiansen and Schmid 2005).

Time Units			Stratigraphic Units	Lithology	Hydrogeology	
Quaternary	Holocene		Surficial deposits	Sand, Silt clay	Aquitard	
		Late Pleistocene	Wisconsinan	Late	Battleford Fm.	Diamicton
	Middle			Floral Fm.	Weathered Zone	
	Early		Upper Till		Diamicton	Aquitard
	Middle Pleistocene	Illinoian		Riddell Mb.	Silt	
				Lower Till	Sand, gravel	Aquifer
					Diamicton	Aquitard
		Pre-Illinoian			Stratified deposits	Aquifer
				Warman Fm.	Diamicton	Aquitard
					Stratified deposits	Aquifer
Tertiary	Late Pliocene		Dundurn Fm.	Diamicton	Aquitard	
				Stratified deposits	Aquifer	
			Mennon Fm.	Diamicton	Aquitard	
		Empress G.	Stratified deposits	Aquifer		
Bedrock Surface						
Cret.			Snakebite Mb.	Silt and clay	Aquitard	

Fig. 2 Late Tertiary and Quaternary stratigraphy and hydrogeology in southern Saskatchewan area (modified after, Christiansen 1992; Mollard et al. 1998)

A stratigraphic framework for the till and intertill stratified units of the Pleistocene glacial period in southern Saskatchewan (Fig. 2) have been established and classified by Christiansen (1992). The Pleistocene till and intertill stratified deposits have been separated into the Empress (discontinuous, proglacial gravels), and overlying predominantly till of Sutherland and Saskatoon groups (Fig. 2). The Saskatchewan Geological Survey (2003) reported that the glacial sediments in southern Saskatchewan are subdivided into two distinctive but gradational groups; till, laid down directly by the ice, and stratified sediments, deposited in water either in glaciofluvial or glaciolacustrine environments. Glaciofluvial stratified sediments are composed mainly of sand and gravel. These sediments are subdivided into ice-contact stratified drift, deposited beneath or immediately in front of the ice, and outwash sediments, deposited by meltwater streams beyond the ice. Glaciolacustrine sands and silts were deposited in glacial lake deltas, whereas the finer silts and clay settled offshore in the lake basins. Figure 3 shows the glacial landforms of the Quaternary deposits surrounding Luck Lake (Saskatchewan Geological Society 2002). As indicated from this map, Luck Lake lies over glaciolacustrine deposits of sand, silt and clay and is bordered on the north side by hummocky till.

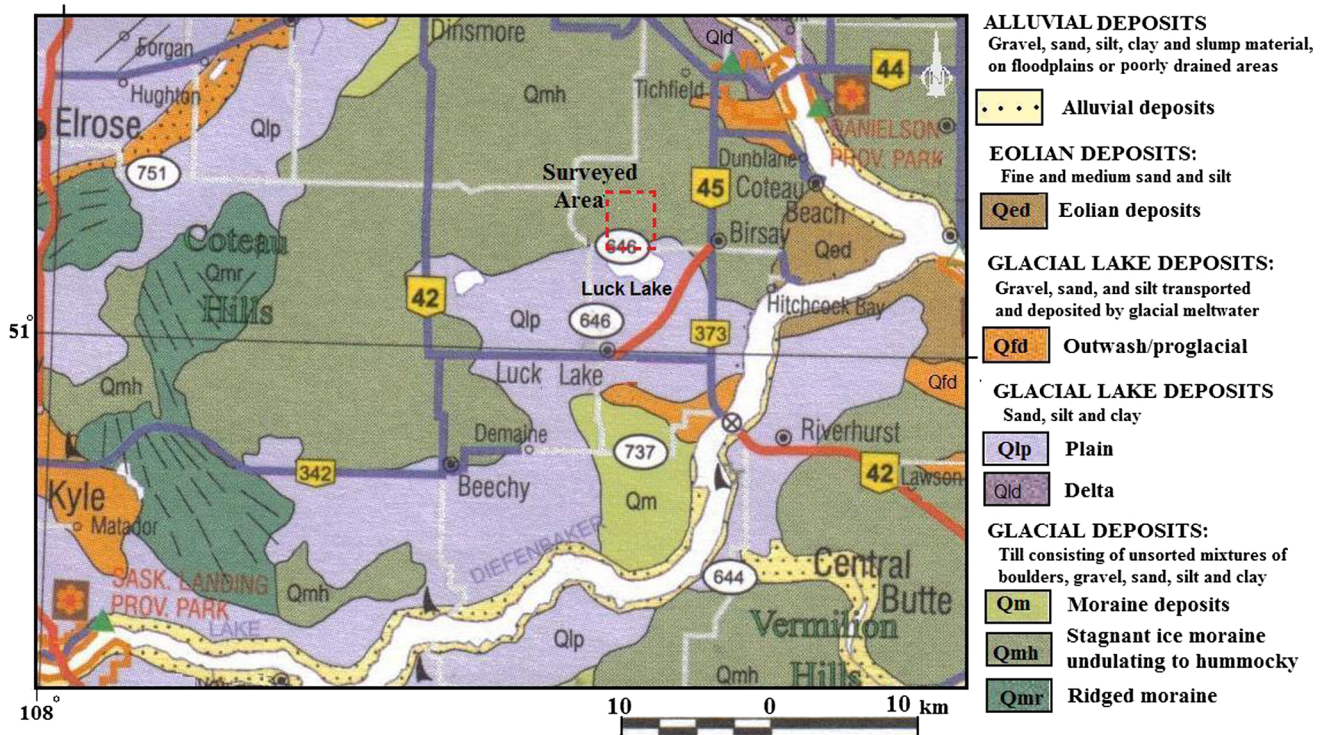
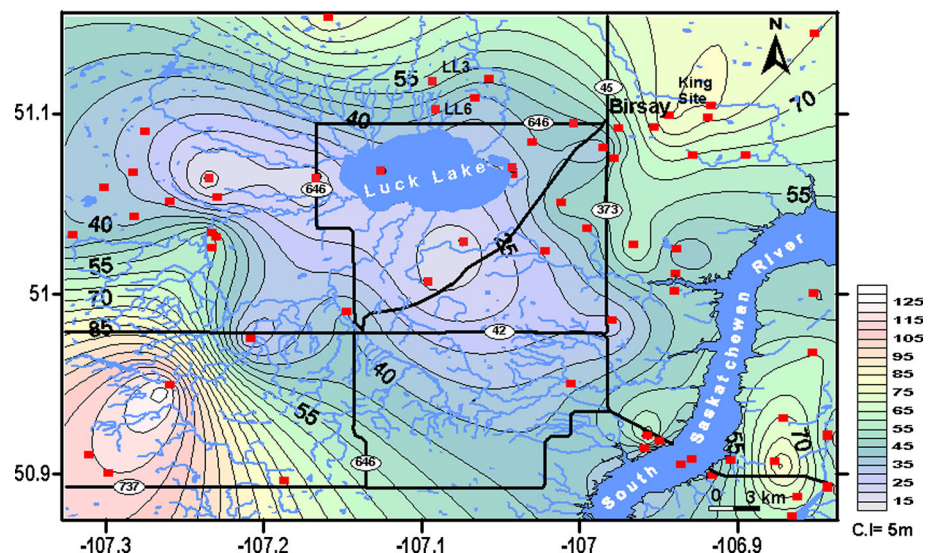


Fig. 3 Surface geological map showing the glacial landforms around Luck Lake area (modified after Saskatchewan Geological Survey 2003)

Fig. 4 Thickness distribution map of the till aquitard around Luck Lake obtained from boreholes



The thickness values of the till deposits were obtained from 62 boreholes around Luck Lake area (Christiansen 1986; Christiansen 1992). The obtained thickness values were interpolated using a kriging algorithm and presented as a contour map of Fig. 4. According to this map, the till in the area ranges in thickness from 14 to 120 m. At borehole LL3, the till aquitard is 55 m thick (Hendry et al. 2011). In the Luck Lake area, Christiansen (1986) identified two till formations capped by Holocene deposits: an

upper oxidized till identified as the Battleford Formation and a basal till called the Floral Formation with thicknesses of 0–5 and 30–70 m, respectively (Hendry et al. 2011). Till in the upper part of the Floral Formation is hard, jointed with yellowish brown and black staining (Christiansen 1992), whereas till in Battleford Formation is soft, massive and unstained. The contact between the Floral and Battleford Formations is unconformable and is marked commonly by a boulder pavement (Fig. 2).

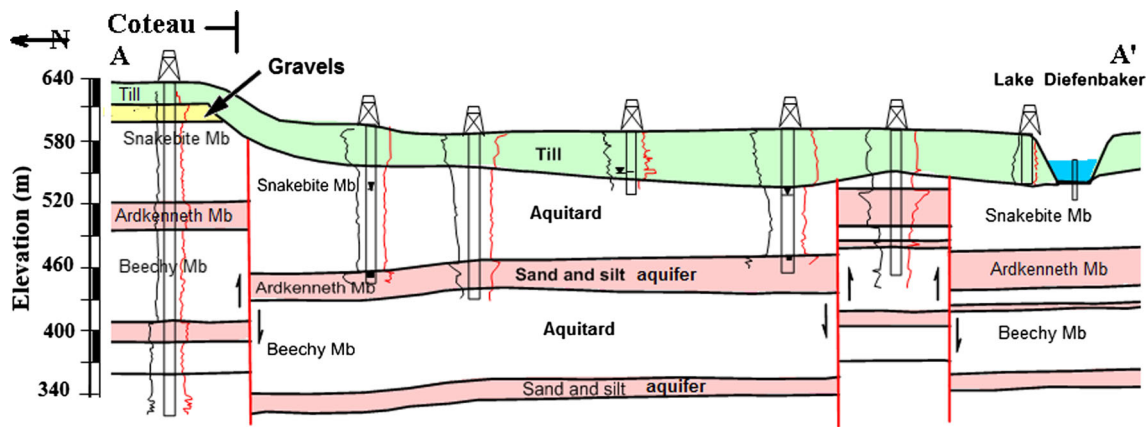


Fig. 5 Geological cross section A-A' shows the stratigraphy and faulting in the area north of Luke Lake. Figure (1) shows the location of A-A' cross-section (modified after Christiansen 1986)

The Saskatoon Group till unconformably overlies the plastic, marine Snakebite Member clay of the Cretaceous Bearpaw Formation (Fig. 5). The glacial and non-glacial overburden, along with the Snakebite Member, forms an aquitard restricting fluid flow into the underlying Ardkeneth sand aquifer.

Hydrogeologically, the till aquitard in the area is typically subdivided into units, a thin layer of brown weathered till below ground surface (5–15 m thick), and follows by grey and commonly thicker unit of unweathered till (Cummings et al. 2012). Weathered till tends to be more permeable than unweathered till and downward groundwater velocities in unfractured are low (Shaw and Hendry 1998). Vertical hydraulic conductivity through unfractured till is 10^{-11} – 10^{-10} m/s (Shaw and Hendry 1998). These values are higher in the coarse-grained materials such as sands and gravels as well as in the presence of fractures in the till drift aquitard.

Powerwater in weathered till is commonly enriched in tritium, Oxygen-18, and deuterium, suggesting that the zone is hydrogeology active (Hendry 1988). The chemistry of the porewater in inter-till sand and gravels aquifers tends to be similar to that of the porewater in the till aquitard (Cummings et al. 2012). The depth to the water table in the Luck Lake area is generally 1–5 m below ground (BG). The shallow depth to water table is attributed to the lack of downward flow due to low vertical hydraulic conductivity of the unoxidized till (Hendry et al. 2011).

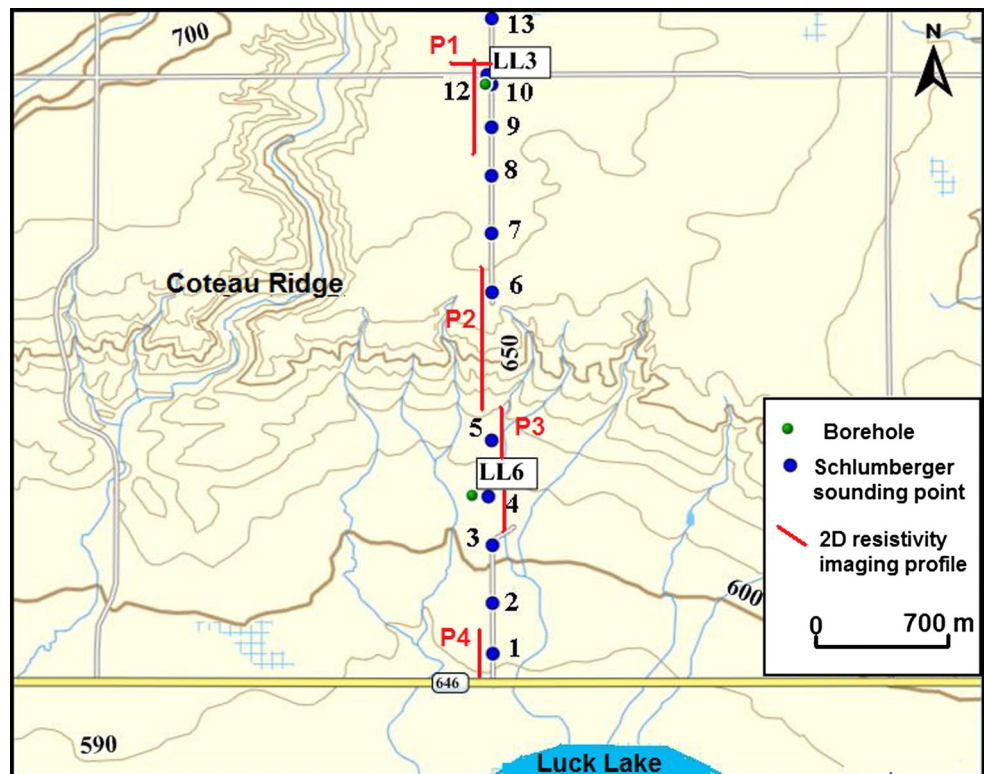
The bedrock, Bearpaw Ardkeneth (aquifer) and Snakebite (aquitard) members are collapsed as a result of dissolution of Devonian salt (Christiansen 1986; Christiansen and Sauer 1998; Cummings et al. 2012). Locally, however, remnants of salt remain as salt horsts (Fig. 5). As shown in the northern end of the cross-section (Fig. 5), the basal part of the till in the footwall of the Coteau ridge is defined by a gravel layer close to the ridge. The vertical displacement in the Snakebite bedrock associated with the collapsed fault is 69 m (Coteau ridge).

Methodology

In the present survey, the resistivity measurements were started by applying the vertical electrical sounding technique (VES). Along a profile between boreholes LL6 and LL3 in the north with 3.6 km length (Fig. 6), 12 Schlumberger sounding points were measured with 1,000 m maximum current spacing (AB). The Schlumberger electrode array was selected due to its advantage with respect to the high penetration depth and its sensitivity for shallow changes. According to the lithologic units obtained from the two boreholes, the applied spread is long enough to penetrate the till glacial drift overburden and reach the Snakebite Member. These soundings were distributed with unequal spacing depending on the civil constructions and topography of the area (Fig. 6). To overcome the ambiguity problem, which is common in the resistivity measurements, two sounding points (VES 10 and 12) were conducted beside borehole LL3 in two different directions. The curves of these soundings show a strong similarity reflecting the same subsurface conditions in both directions. During the Schlumberger data collection, the resistivity meter obtained the apparent resistivity and estimated the standard deviation of errors from repeat cycles. Observations with a standard deviation error of $>0.1 \Omega\text{m}$ were repeated or discarded.

The measured sounding points were inverted using IP2WIN (Bobachev et al. 2003). The inversion procedure in this program is based on a linear filtering algorithm, which provides a fast and accurate direct problem solution for a wide range of models, covering all reasonable geologic situations. To select the model that best represents the true conditions of the subsurface, lithology and depths of subsurface layers from borehole LL3 were used to fix some layer parameters to obtain the actual resistivity values (Fig. 7). All soundings along the profile were treated as a unit based on the lithologic boundaries obtained from

Fig. 6 Location map of the resistivity measurements in the north of Luck Lake area. *P* are locations of Wenner spreads. Elevation contour intervals are 10 m



boreholes LL3 and LL6 to represent the variations in the subsurface geological conditions.

Four 2D resistivity profiles were measured along the long intersect that intercepts boreholes LL3 and LL6. In this technique, the resolution of the resistivity imaging method is controlled by the electrode spacing, the type of array used, and the noise levels and by the local geology (Beresnev et al. 2003). Before the field measurements, different electrode arrays were tested using a synthetic forward model obtained from the available geological information and the Schlumberger sounding survey. The tested arrays were included dipole–dipole, Wenner, pole–dipole and pole–pole arrays. Based on this information, a Wenner array was selected for the resistivity imaging survey where the inverted model of this array provides an approximate guide to the geometry and true formation resistivity (Dalhin and Zhou 2004). In addition, the Wenner array is characterized by greater investigation depth compared with the dipole–dipole array. On the other hand, the dipole–dipole array has good imaging resolution at shallow depth and can be used to detect rapid changes of the upper parts of overburden till but it has a very low signal-to-noise ratio at high data levels, $n = 6$ (Dalhin and Zhou 2004). These conditions reflect the reliability of Wenner array to detect the vertical variations and heterogeneity of the till overburden.

The apparent resistivities were collected along the profiles using 30 electrodes system with 10-m minimum

electrode spacing and data level $n = 10$. These parameters allow for imaging of the variations in the subsurface conditions to a depth of 50 m using Wenner array. A Syscal Jr. with 30 Smart Nodes cable was used to automate the data collection as much as possible.

The apparent resistivity pseudosections were processed and inverted using the smoothness-constrained least-squares method (Loke and Barker 1996) to create true resistivity sections. The inversion procedures in this technique are carried out using a non-linear least-squares optimization algorithm to fit the measured resistivity values (Loke and Barker 1996). The elevations along the measured lines were included during the inversion process. The inversion parameters were set based on expected subsurface geology, quality of measured data, type of electrode array and expected resolution of the inverse models. The resulting inversions were compared with the original input models obtained from the results of Schlumberger soundings and geological information from LL3 and LL6 boreholes. In general, the inversions gave relatively high-resolution images and revealed that the geometries of the resistivity anomalous areas were sufficiently recovered.

Results and discussion

The results of the Schlumberger soundings were correlated with lithologic units from boreholes LL3 and LL6

Fig. 7 Correlation between the interpreted 1-D model of sounding 10 and the Single Point Resistance and SP logs of borehole LL3

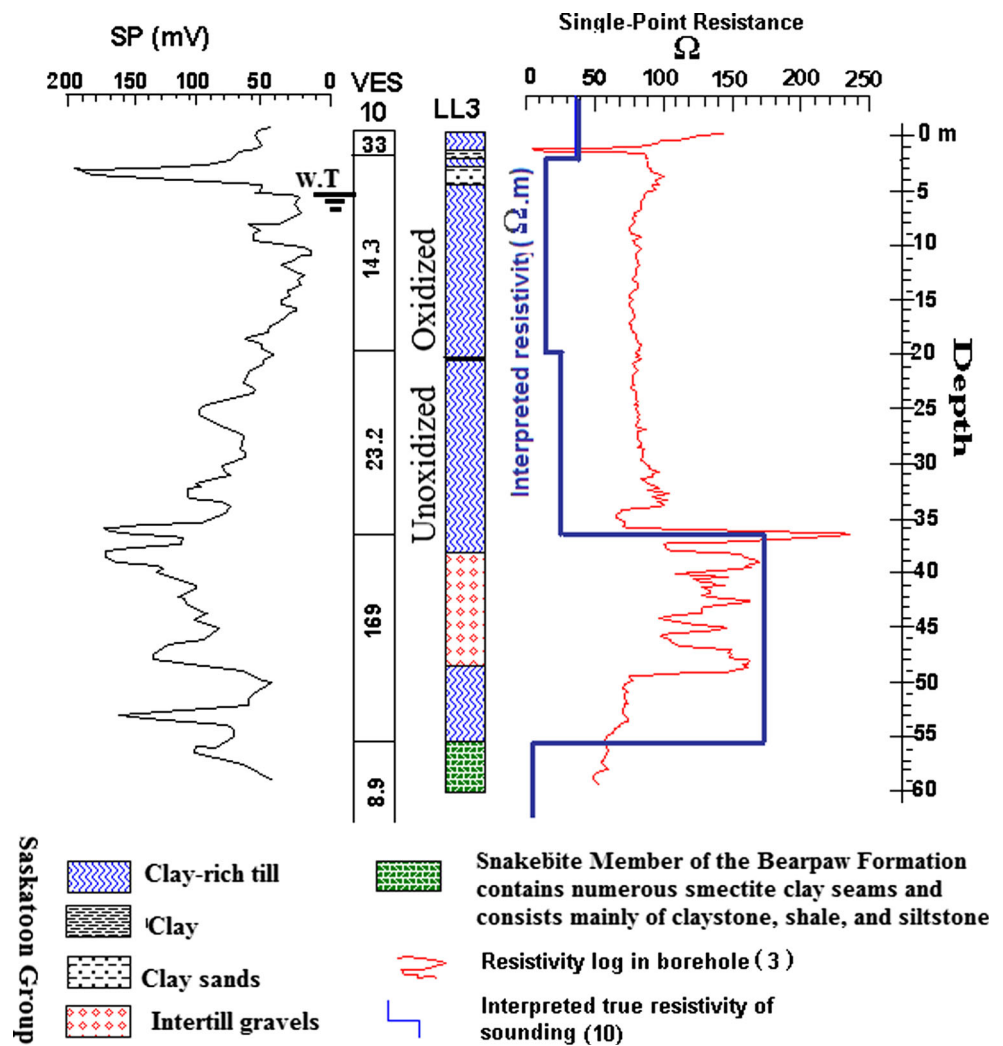


(Table 1). The obtained geoelectrical layers were used to generate the geoelectrical cross-section in Fig. 8. The apparent resistivity section (Fig. 8a) shows considerable variations in the apparent resistivity distributions on both sides of the fault zone, which is in the area between soundings 5 and 6. The hanging wall of the fault is characterized by relatively low apparent resistivity values (2–10 Ωm) compared with the footwall side. A lens-shaped resistive zone in the basal part of the footwall is interpreted to be gravel and sand. This high resistive zone (>100 Ωm) is increased in resistivity and thickness towards the ridge near sounding six reflecting greater thickness of the gravel.

The interpreted sedimentary textures and location of the fault are presented in Fig. 8b. On the whole geoelectrical section, the relatively low resistivity values (2–9 Ωm) in the lower part permitted to clearly identify the depth of shale bedrock of Snakebite Member.

In the footwall, the deeper part (at depth of 35 m) has a resistivity range between 169 Ωm at borehole LL3 and

>500 Ωm near the ridge slope. This great variation in the resistivity may be due to variable grain size, fracture quality and water content, or lack of it, in this gravel stratum. This gravel stratum is considered as intertill or stratified ice-contact deposits in the till aquitard and exposed in some pits along higher elevations in the ridge zone (between sounding 5 and 6). The thickness of the gravel stratum is decreased gradually towards sounding 11 in the north direction and is not evident in the hanging wall of the Coteau ridge. These till deposits are considered as glaciofluvial deposits and are characterized by high resistivity values compared with sediments in the hanging wall.

In the hanging wall, the till deposits show low resistivity values of 15–41 Ωm due to the increasing amount of lacustrine clays, silt and gypsum as indicated from Borehole LL6. These deposits are characterized by glaciolacustrine facies. The lower part of the till deposits shows a high resistivity values (20–46 Ωm) compared with the upper zone to indicate the unoxidized zone. The depth to

Table 1 Resistivities and thicknesses of the geoelectrical layers and its geological interpretation

VES no.	Elevation (m)	Resistivities (Ω m)					Thicknesses (m)				Depth to bedrock	Boreholes	
		P1*	P2*	P3*	P4**	P5***	h_1	h_2	h_3	h_4			
1	592	1.7	4.2	33.4		2.9	4.28	17	30.65	51.94		Hanging wall	
2	592	8.4	4.2	44		2.8	2.9	21.1	28.52	52.4			
3	600	3.3	9.5	36.2		6.51	8.06	20.8	12.6	41.5			
4	599	30.7	7.7	36.2		4.34	1.66	23.5	17.76	42.9		LL6	
5	607	24.6	11.7	33		6.09	4.54	20.8	19.2	44.5			
6	681	18.9	45.4	15.7	545	6.43	1.12	2.5	23.53	28	55.71		Foot wall
7	689	16.7	24.2	18.3	462	2.11	1.02	1.75	35.8	24.9	63.2		
8	681	51.3	13.8	19.8	463	5.5	1.39	2.39	29.71	19.2	52.74		
9	682	104	26.5	17.9	366	6.19	1.51	13.8	18.26	21.8	55.4		
10	687	34.1	14.3	23.2	169	8.95	2.1	17.5	17.42	18.4	55.51		LL3 (NS)
11	690	18.7	12.3	22.3	88	6.81	3.61	4	34.16	16.5	57.26		
12	687	24.3	14.6	23	153	8.7	2.15	17.5	17.4	18.4	55.4		LL3 (EW)

Lithologic description: * P1, P2, P3 Glacial tills, lacustrine clays, claystones (Saskatoon Group), ** P4 Sand and gravels, *** P5 Snakebite Member of the Bearpaw Formation contains numerous smectite clay seams and consists mainly of claystone, shale, and siltstone

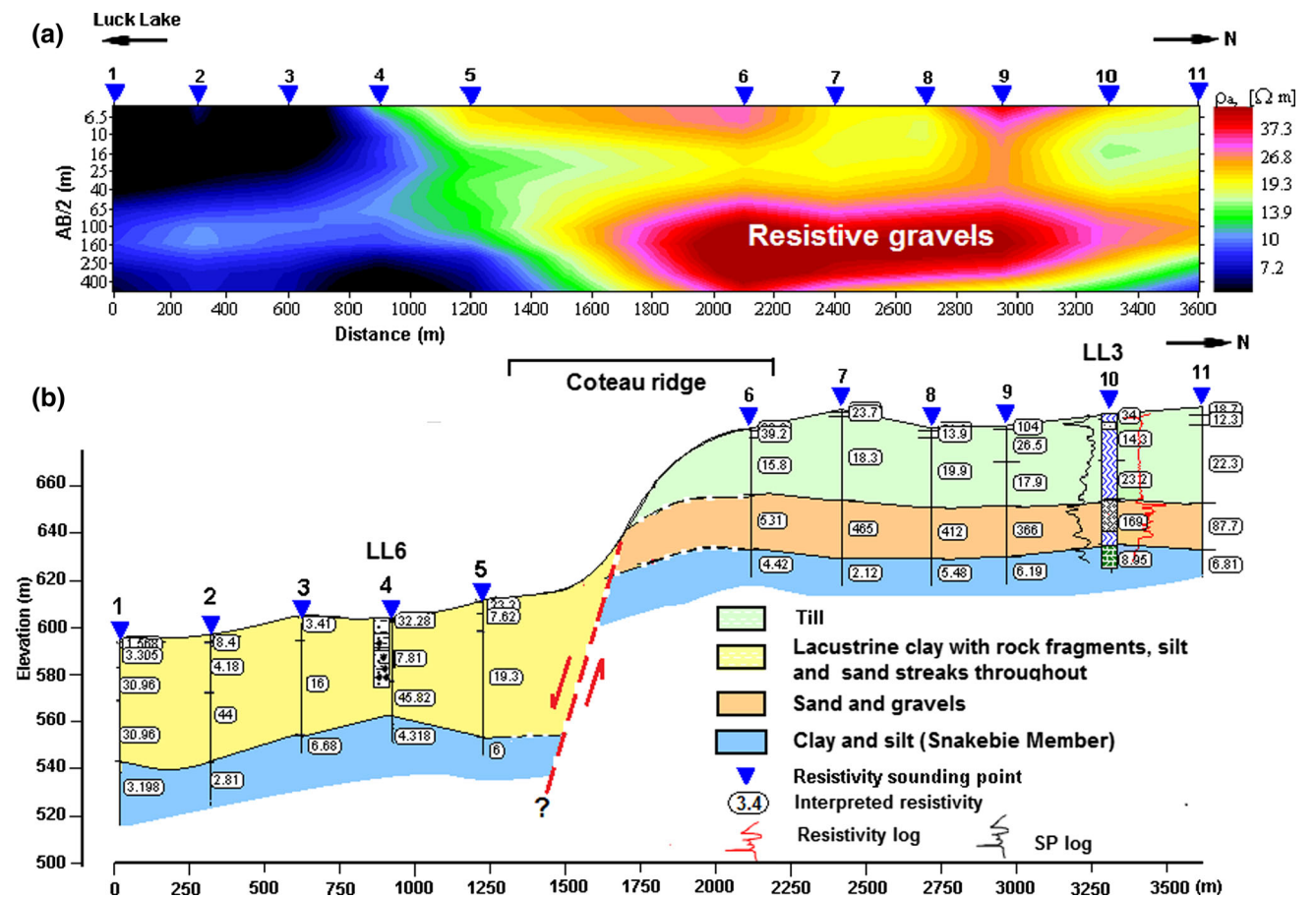


Fig. 8 The apparent resistivity section and geoelectrical cross section along the profile between LL3 and LL6

the bedrock (Snakebite Member) varies between 42 and 53 m in the lowland area and from 53 to 63 m in the upland area (Table 1).

The overburden till has been investigated in detail using the inverted 2D resistivity imaging sections collected in Wenner array form. To show the continuity of gravel

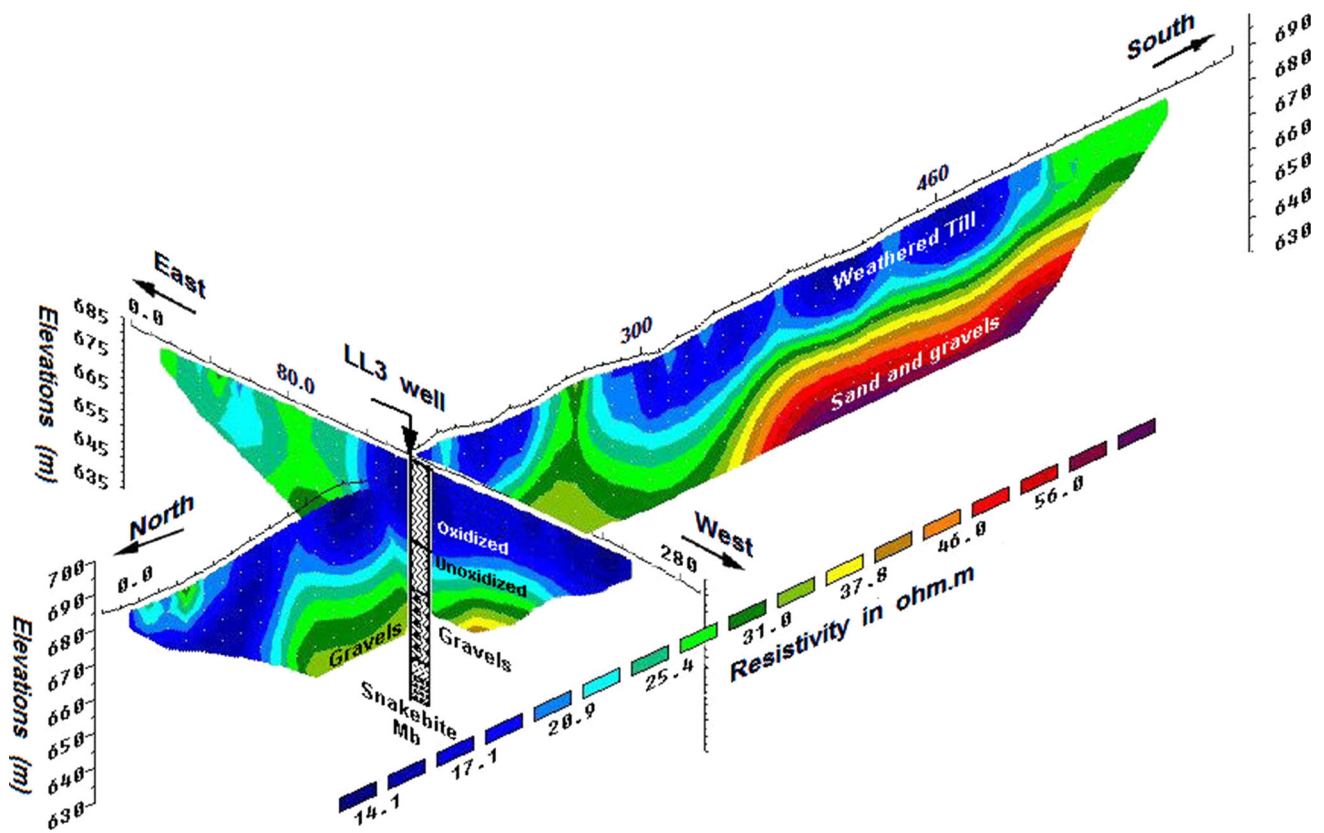


Fig. 9 2-D Wenner inverted sections (P2) around borehole LL3 showing the gravel in the basal part of the till and extending towards the south

materials around LL3, the inverted section along P1 was compiled with its perpendicular line (Fig. 9). This profile runs in north–south direction with 620 m length. Around the borehole LL3, the gravel materials showed low resistivity values (31–37 Ωm) compared with higher resistivity zone (150 Ωm) towards the southern side. The well-defined high resistivity zone was interpreted as a till with large gravel boulders. The upper low resistivity zone (<20 Ωm) corresponds to weathered and fractured till (oxidized till), which extends to 15 depth. Below this low resistivity zone, a relatively more resistive zone (20–50 Ωm) is observed over basal gravel stratum. This zone corresponds to unweathered till. Shaw and Hendry (1998) described the lower part of the till as soft, massive, and dark olive gray, whereas the upper part of the till is soft, brown, oxidized, and visibly fractured.

To understand the resistivity distributions resulting from the discontinuity of the gravel stratum along the fault zone, a synthetic resistivity model was created using the same field parameters as 10 m electrode spacing and Wenner array. As shown in Fig. 10a, the geological model simulates a 10 m thick gravel and sand stratum interbedded in the till that terminates at the fault zone (Coteau ridge). The shale bedrock (Snakebite Member) is apparent in the basal part of the model and is affected by the fault (Fig. 10a).

The resistivity ranges of the synthetic model were inferred from the former sounding survey and the parametric measurements near the boreholes LL3 and LL6. The synthetic modeling process was started by calculating the apparent resistivity distributions along the obtained geological model using the 2D forward modeling program (Loke and Barker 1996). The apparent resistivity calculations were carried out using finite-difference method and exported as a data file with added 5 % random noise (Fig. 10b). The calculated synthetic model was inverted to display the resistivity patterns along the fault zone (Fig. 10c). During the inversion procedures, the inversion parameters were adjusted to image the suggested geological model. Figure 10c shows the final inverted model after five iterations and its geological interpretation.

The second measured Wenner 2D profile (P2) was compared with the inverted synthetic model (Fig. 10c) to define the resistivity patterns along the Coteau ridge. This profile (Fig. 11) runs crossing the fault zone with 900 m length. The inverted section of P2 shows the same well-defined interface between upper till zone and the gravel stratum in the footwall side and is not present in the hanging wall area. This facies changes dramatically on the hanging wall of the fault plane with relatively low resistivity sediments interpreted to be clay-rich sediment and

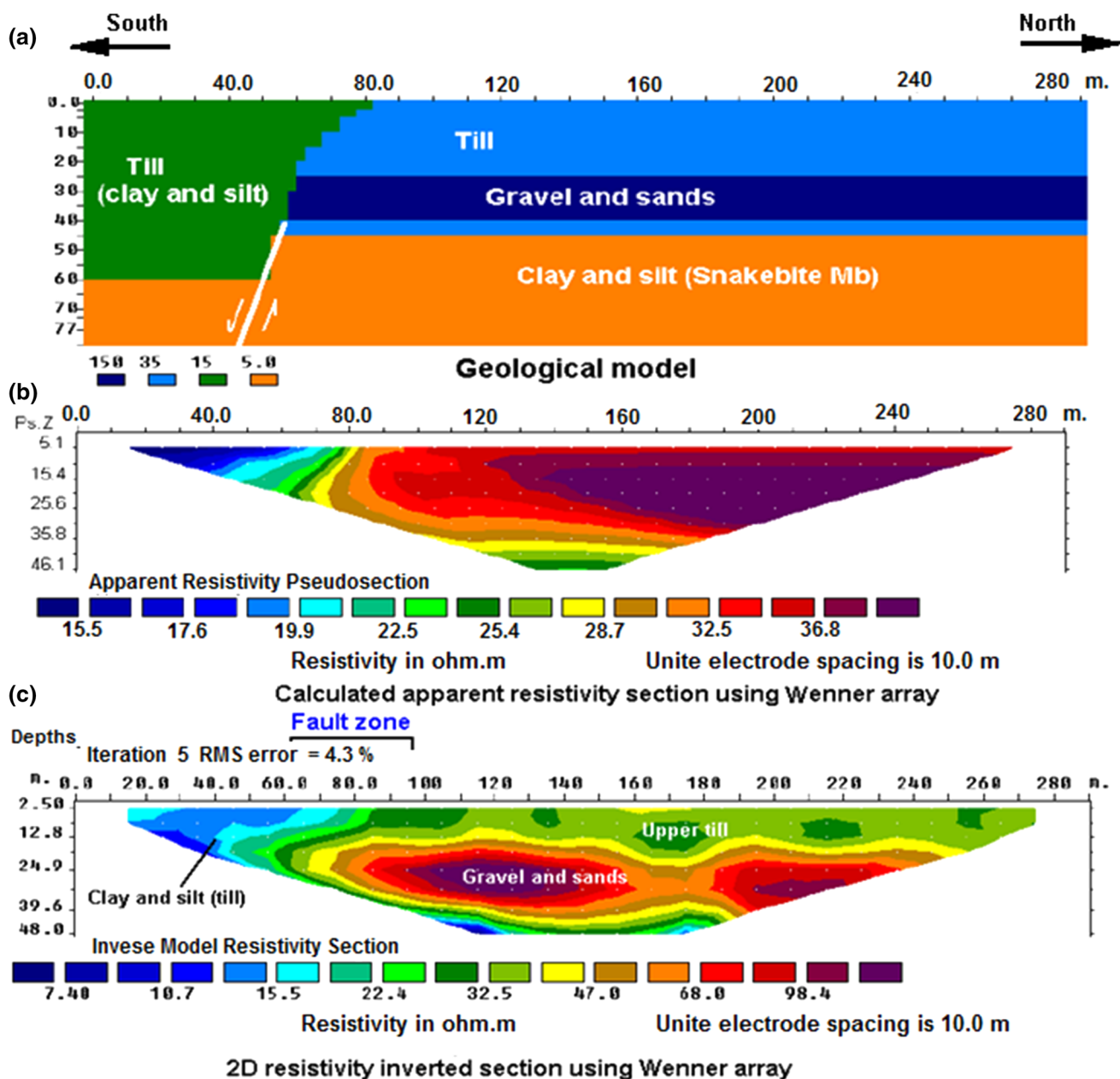


Fig. 10 2-D synthetic model using Wenner array shows the resistivity patterns resulting from gravels with till background crossing the fault zone

shallow shale bedrock along the fault plane. The basal gravel stratum shows a higher resistivity ($>300 \Omega\text{m}$) and thickness near the ridge in the footwall side. The elongated conductive features appeared in the top 15 m of the section are attributed to an intensely fracture zone filled with clays or water. This profile clearly illustrates the lateral and in depth extent of the resistive and conductive anomalies observed in the till overburden on both sides of the ridge. Two-dimensional imaging resistivity survey has proven to be useful for mapping the lateral and vertical variations in the till overburden. The multi-electrode system, with 30

electrodes spaced at 10 m, provided good resolution in the upper 50 m. However, this system was not suitable for identifying the bedrock surface in the upside area due to its limited penetration depth.

Profile P3 is located in the vicinity of borehole LL6 and has 900 m length (Fig. 12). Along this profile, the high resistivity anomalies within the overburden reflect the heterogeneity of the constituents where it consists of eroded materials from the high land (sand, gravel pebbles and silt). The Snakebite Member appears in the middle part of P3 at depths varying between 40 to 50 m with low

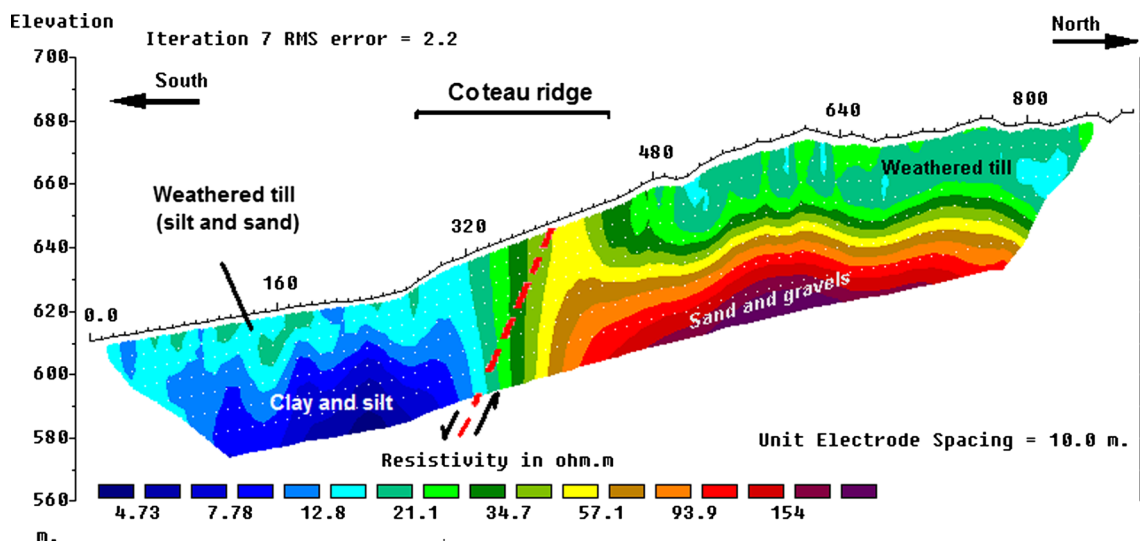


Fig. 11 2-D Wenner inverted section (P2) crossing the fault zone and showing the gravel in the basal part north of the ridge. The interpreted fault zone lies between stations 300 and 400 m N

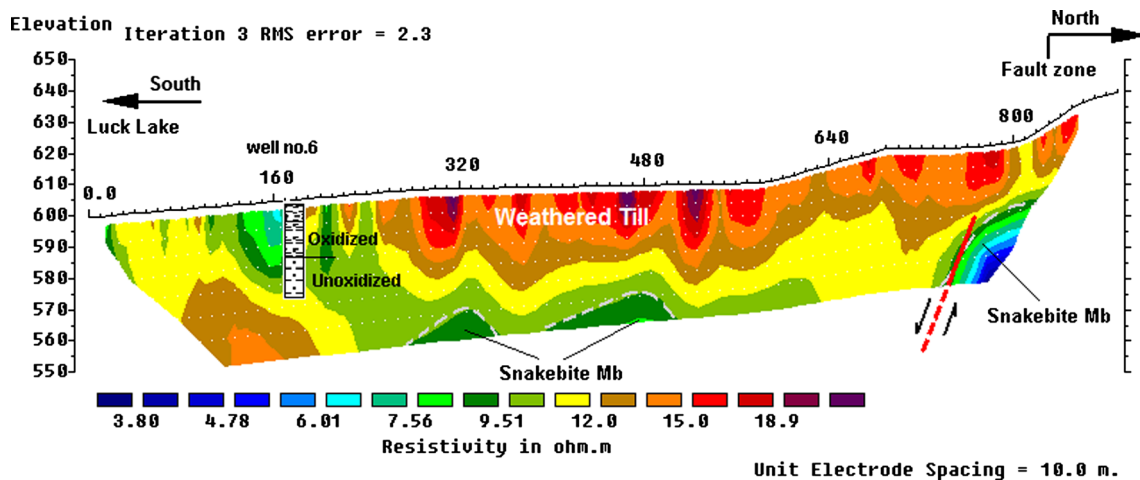


Fig. 12 2-D Wenner inverted section (P3) around LL6 borehole in the hanging well of the fault zone. The *dashed line* represents the interpreted bedrock surface. The *red line* in the lower-right corner of the inverted section represents the fault line

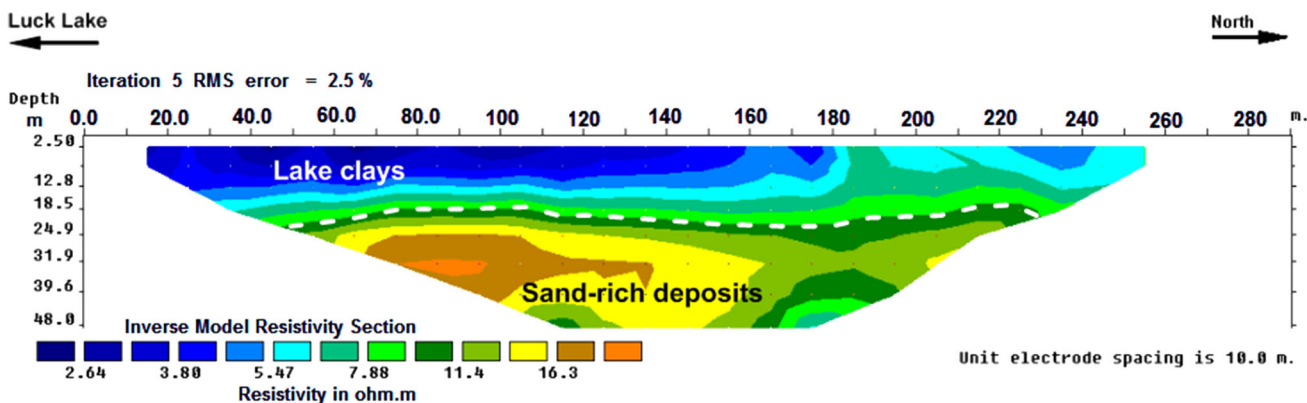


Fig. 13 2-D Wenner inverted section (P4) close to the Luck Lake. The *dashed line* represents the interpreted boundary between the clay-rich till and sand-rich till

resistivity values ($<6 \Omega\text{m}$). The fault line is interpreted at depth of 25 m in the northern end of this profile, where the Snakebite bedrock of low resistivity appeared as sharp contacts with till overburden (Fig. 12). In the overlap area between P2 and P3, the gravels appear in some pits along the fault zone. At borehole LL6, the oxidized till is observed as a conductive sediment with 6–8 Ωm resistivity range at a depth of 15 m.

Along the closest 2D Wenner profile (P4) to Luck Lake, the topography has only a gentle slope and hence no topographic correction was completed. The resistivity distribution in P4 has low resistivity contrasts ranging from a minimum of 2 Ωm to a maximum of 20 Ωm with data to a depth of 50 m (Fig. 13). The gravel and coarse-grained sand deposits are absent in the hanging wall block. Changes in the resistivity signal are interpreted to represent two till layers; an upper oxidized till zone with low resistivity ($<7 \Omega\text{m}$) interpreted to be clay-rich glaciolacustrine deposits and a lower layer with more sand and silt and resistivity in the range 8–20 Ωm . The thickness of the upper zone varies from 15 to 20 m towards the lake.

Summary and conclusions

This study illustrates that resistivity surveying is a practical and non-invasive tool that can be used to image the intertill gravels across the north ridge of Luck Lake. The resistivity imaging survey allowed for the study of geological structure of the till deposits in the area. The results of the resistivity sections illustrated that the till lithologies change dramatically from one side of the ridge to the other. The gravels of the footwall are blanketed by discontinuous till and lacustrine clay dominates in the hanging wall parts around Luck Lake. Calibration at the borehole site with known thickness of gravel stratum indicated that the resistivity of gravel materials could lie within the range of 80–500 Ωm , depending on the seasonal variation in groundwater levels. The resistivity sections indicated that the resistivity and thickness of the gravel increase towards the ridge. The presence of this coarse-grained sediment and the fractures in the top of till overburden increase the total hydraulic conductivity of the aquitard and may provide preferential pathways for surface waste disposals.

The geological interpretation of resistivity sections indicated that the till aquitard in the area consists of 60 m of plastic clay-rich till of Battleford till. The good resistivity contrasts between clay-rich overburden ($<30 \Omega\text{m}$) and glacial gravels ($>300 \Omega\text{m}$) were observed in all 1-D and 2D sections. The upper 15 m of till is oxidized and fractured with low resistivity values (14–20 Ωm) whereas the rest is unoxidized and unfractured. The resistivity

sections showed a strong resistivity contrast between the sand and gravel and late Cretaceous clay bedrock ($<6 \Omega\text{m}$).

The results of this study will help for additional studies regarding depositional and hydrogeological modeling to study the impact of gravels, fractures and fault systems that can control the percolation of surface contaminants in the till aquitard. The interpreted gravel layer, along the measured 2D profiles could be used to construct a stratigraphic model integrated with the conceptual environmental and depositional models along both sides of the Coteau ridge to define its origin and discontinuities in the whole area. As indicated from the available boreholes, these intertill gravel deposits extend in the eastern side of the surveyed area and represent stratified sediment or ice-contact deposits in the till overburden.

Acknowledgments I wish to thank M. J. Hendry, Department of Geological Sciences, University of Saskatchewan, for his financial support of the field work through his NSERC Industrial Research Chair. Also, I would like to thank Jim Merriam, professor of Geophysics at University of Saskatchewan, Canada for his careful review of the manuscript as well as his kind supporting during the field works. This paper benefited from comments provided by all selected reviewers.

References

- Aizebeokhai AP (2009) Geoelectrical resistivity imaging in environmental studies. In: Yanful EK (ed) *Appropriate technologies for environmental protection in the developing world*. Springer, Netherlands, p 305. doi:10.1007/978-1-4020-9139-1_28
- Beresnev IA, Hruba CE, Davis CA (2003) The use of multi-electrode resistivity imaging in gravel prospecting. *J Appl Geophys* 49:245–254
- Bobachev A, Modin I, Shevinin V (2003) IP2WIN V2.0: user's guide. Moscow state University, Geology Faculty, Geophysics Department, p 46
- Boris, M (2005) Azimuthal resistivity to characterize fractures in the Battleford formation. Birsay, Saskatchewan. M.Sc thesis, Department of Geological Science, Saskatchewan University, http://library2.usask.ca/theses/available/etd-02232006-152036/unrestricted/m_boris.pdf
- Boris M, Merriam JB (2002) Azimuthal resistivity to characterize fractures in glacial till; Symposium on the Application of Geophysics to Environmental and Engineering Problems, Las Vegas, Nevada, p 10
- Chambers JE, Wilkinson PB, Weller A, Meldrum PI, Kuras O, Ogilvy RD, Aumonier J, Bailey E, Griffiths N, Matthews B, Penn S, Wardrop D (2012) Characterising sand and gravel deposits using electrical resistivity tomography (ERT): case histories from England and Wales. In: Hunger E, Walton G (eds) *Proceedings of the 16th Extractive Industry Geology Conference*, EIG Conferences Ltd, pp 166–172
- Christiansen EA (1986) *Geology of the Luck Lake Irrigation Project*, Report 0114–002. E.A Christiansen Consulting Ltd., Saskatoon
- Christiansen EA (1992) Pleistocene stratigraphy of the Saskatoon area, Saskatchewan, Canada; an update. *Can J Earth Sci* 29(8):1767–1778
- Christiansen, Sauer (1998) *Geotechnique of Saskatoon and surrounding area*, Saskatchewan, Canada. In: Darrow PF, White OL (eds)

- Urban geology of Canadian cities. *Geol Assoc Can Spec Pap* 42:117–145
- Christiansen EA, Schmid BJ (2005) Glacial geology of southern Saskatchewan. *Proceedings of the 58th Canadian geotechnical conference*, vol 2, September 18–2, 2005, Saskatoon, Saskatchewan, Canada
- Cummings DI, Russell HA, Sharpe DR (2012) Buried valleys and tills in Canadian Prairies: geology, hydrogeology and origin. *Geological Survey of Canada, Current Research* 2012–4, p 22. doi:10.4095/289689
- Dalhin T, Zhou B (2004) A numerical comparison of 2D resistivity imaging with 10 electrode arrays. *Geophys Prospect* 52:379–398
- Gemal KS (2012) Monitoring of wastewater percolation in unsaturated sandy soil using geoelectrical measurements at Gabal el Asfar farm, Northeast Cairo, Egypt. *Environ Earth Sci* 66(3):749–761
- Haefner RJ (2000) Characterization methods for fractured glacial tills. *Ohio J Sci* 100(3–4):73–87. <http://hdl.handle.net/1811/23858>
- Hendry MJ (1988) Hydrogeology of clay till in Prairie region of Canada. *Groundwater* 26(5):607–614
- Hendry MJ, Ranville J, Boldt-Leppin BEJ, Wassenaar LI (2003) Geochemical characteristics and transport of DOC in a clay-rich aquitard. *Water Resour Res* 39(7):1194. doi:10.1029/2002WR001943
- Hendry MJ, Kotzer T, Solomon DK (2005) Sources of radiogenic helium in a clay till aquitard and its use to evaluate the timing of geologic events. *Geochim Cosmochim Acta* 69(2):475–483
- Hendry MJ, Barbour SL, Zettl J, Chostner V, Wassenaar LI (2011) Controls on the long-term downward transport of d_2H of water in a regionally extensive, two-layered aquitard system. *Water Resour Res* 47:W06505. doi:10.1029/2010WR010044
- Loke MH, Barker RD (1996) Rapid least-squares inversion of apparent resistivity pseudosections by a quasi-Newton method. *Geophys Prospect* 44:131–152
- McCombie C (1997) Nuclear waste management worldwide. *Phys Today* 50(6):56–62
- Mollard J, Kozicki P, Adelman T (1998) Some geological, groundwater, geotechnical and geoenvironmental characteristics of the Regina area, Saskatchewan, Canada. In: Darrow PF, White OL (eds) *Urban geology of Canadian Cities*, *Geol Assoc Can Spec Pap* 42, pp 147–170
- Phillips OM (2009) *Geological fluid dynamics: sub-surface flow and reactions*. Cambridge University Press, Cambridge, p 285
- Remenda VH (1993) Origin and migration of natural groundwater tracers in thick clay tills of Saskatchewan and the Lake Agassiz clay plain. unpublished Ph.D. thesis, Univ. Waterloo, Waterloo, ON, p 273
- Saskatchewan Geological Society (2002) *Geological Highway Map of Saskatchewan*, 1st edn. *Sask Geol Soc Spec Publ No. 15*, map with marginal notes
- Saskatchewan Geological Survey (2003) *Geology, and Mineral and Petroleum Resources of Saskatchewan*. *Sask. Industry Resources, Misc Rep* 2003–7, p 173
- Shaw RJ, Hendry MJ (1998) Hydrogeology of a thick clay till and Cretaceous clay sequence, Saskatchewan, Canada. *Can Geotech J* 35:1041–1052
- Smith RC, Sjogren DB (2006) An evaluation of electrical resistivity imaging (ERI) in Quaternary sediments, southern Alberta, Canada. *Geosphere* 2(6):287–298
- Van Stempvoort DR, van der Kamp G (2003) Modeling of hydrochemistry of the aquitards using minimally disturbed samples in radial diffusion cells. *Appl Geochem* 18:551–565
- Ward SH (1990) Resistivity and induced polarization methods. In: Ward SH (ed) *Geotechnical and environmental geophysics, Part 1*, publisher, pp 147–190
- Griffiths DH, Barker RD (1993) Two-dimensional resistivity imaging and modelling in areas of complex geology. *J Appl Geophys* 29:211–226